

Applications of Brownian motors

Heiner Linke

Physics Department and Materials Science Institute, University of Oregon

Eugene, OR 97403-1274, USA

ABSTRACT

Brownian motors combine asymmetry (such as a ratchet potential) and stochastic (thermal) motion with non-equilibrium processes to generate directed particle flow. A brief general introduction to Brownian motors is given, and the relevance of the ratchet model for biological motor proteins is highlighted. However, the impact of research on Brownian motors goes far beyond biophysics. A wealth of novel phenomena has been predicted, and some of these phenomena have been observed in areas as diverse as synthetic chemistry, bio-molecular colloids, self-organizing systems, quantum electronics, micro-fluidics, and materials science. Applications, such as novel actuators and molecular separation techniques, are evolving quickly. In the oral presentation, I will attempt to give an overview on applications of ratchets and Brownian motors. In the present paper, I give a short overview and review then a recent experimental realization of a tunneling ratchet for electrons. Such electron tunnelling ratchets can not only be used to generate *particle* currents, but also to pump *heat*. Using a realistic model, the heat pumping properties of the experimental electron ratchet are analysed.

Keywords: Brownian motor, ratchet, quantum ratchet, mesoscopic, heat pump

1. INTRODUCTION

Imagine a nanometer sized car engine with a piston the size of a large molecule. Imagine further that all engine parts are surrounded by water, and that the chemical energy available for each engine cycle is only a few times the ambient thermal energy, $k_B T$. An engineer attempting to build such an engine would face at least two fundamental problems. Firstly, the piston, and all its surrounding parts, are constantly subject to thermal noise (Brownian motion) of order $k_B T$, disturbing the action of the piston. Secondly, inertia, crucial for the function of a conventional, man-made engine, is in effect non-existent for this engine - the viscosity of water stops a moving, submicron particle within a distance much smaller than the particle dimension [1, 2].

The significance of the above scenario is the environment in which biological molecular motors operate. Molecular motors are large protein assemblies inside living cells that perform mechanical tasks such as exerting force (for instance in a muscle or during cell partition), pumping ions across membranes, transporting materials in cells, and transcribing DNA [3]. Motor proteins have a typical mass of the order of 10^3 atomic units, a mass density comparable to water, and are immersed in aqueous solution at body temperature. The chemical energy available per motor cycle from the hydrolysis of adenosine-triphosphate (ATP) is about $14 k_B T$, only one order of magnitude larger than the ambient thermal noise. In spite of these advert operating conditions, natural molecular motors have been shown to transduce chemical into mechanical energy with an efficiency in the 50% to 100% range [4, 5], rather

higher than that of macroscopic, man-made engines. How does Nature achieve this feat of operating a machine efficiently in an overwhelmingly noisy environment?

The so-called thermal ratchet model suggests that molecular motors, rather than *overcoming* noise, *make use* of random thermal motion to generate directed motion [6-13].

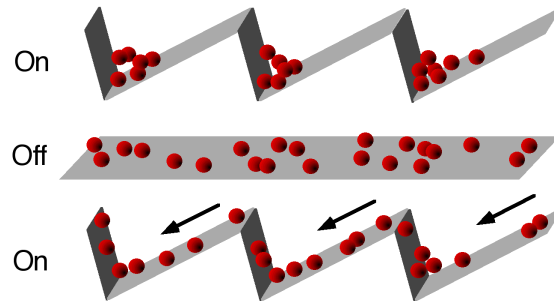


Fig. 1. A pulsating ratchet. During the on-phase, Brownian particles concentrate around the potential minima. During the off-phase, the particles diffuse isotropically. Periodic or stochastic switching between both states induces a particle current to the left (Illustration from [14]).

Fig. 1 shows an illustrative example for one type of a ratchet, namely a so-called pulsating ratchet (also called flashing ratchet) [10, 15, 16]. In this system, Brownian particles are subject to a time-dependent, asymmetric, periodic potential. In the simplest case, the potential can be in one of two states, either flat (off) or saw-tooth shaped (on). If the potential is permanently either off or on, the system is in thermal equilibrium and particles diffuse isotropically. However, when the potential is off at first, and is then suddenly switched on, particles will during a transient period of time move towards the closest local potential minimum. Due to the asymmetry of the saw-tooth potential, the nearest minimum is on average to the left of the particle. Periodic or stochastic switching of the potential (on a time scale comparable to the diffusion time between neighboring potential minima) will therefore result in a net particle flow towards the left, although no net force acts on the particles (for an illustrative Java applet, see [17]). When the parameters are well-chosen, the current can flow against a small external force, in which case the ratchet extracts useable work from the switching potential. Interestingly, while excess thermal noise will render the ratchet process inefficient, the ratchet *needs* thermal particle motion to operate — at zero temperature, the ratchet would not work. In other words, rather than losing efficiency because of the noisy environment, the ratchet makes use of random thermal motion, using external energy.

As a general definition, a ratchet is a system in which asymmetry and non-equilibrium combine to generate directed particle flow in the absence of any macroscopic net (time-averaged) forces or gradients. In the example of a pulsating ratchet given above (Fig. 1), the required asymmetry is represented by the shape of the potential, defining a preferred direction of motion, while the switching of the potential provides the necessary source of non-equilibrium energy. Each time the potential is switched on particles are lifted up, and external energy is transferred to the particle system. Unless the system is coupled to a thermal bath, the particle gas will heat up.

A second example is the so-called rocking ratchet, consisting of particles in an asymmetric potential that is periodically and symmetrically tilted or rocked (Fig. 2). The effective height of each potential barrier changes upon tilting of the potential, and is lower for tilt towards the gentler slopes of the barriers (to the right in Fig. 2). In the simplest case, when only thermal excitation over the barriers is taken into account (while quantum effects, such as tunnelling through the barriers, is neglected), a net current to the right will be observed after averaging over both tilt

directions, because thermal excitation of particles over the barrier is more probable during tilt to the right when the effective barrier height is lowest [6, 18].

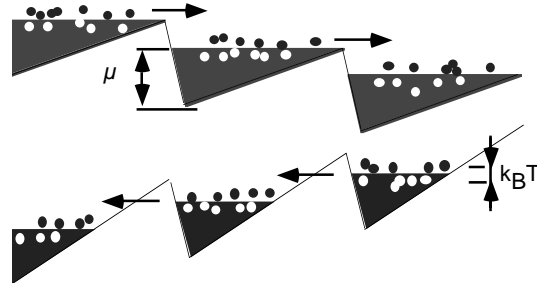


Fig. 2. A rocking ratchet. The indicated energy distribution of the particles assumes fermions (Fermi energy μ , temperature T). The ratchet potential is tilted symmetrically and periodically. Due to the asymmetry of the barriers, the currents induced during the two halfcycles are different, and, averaged over a full cycle, a net current occurs. In the situation shown here, the barrier height is lower for tilt to the right. Tunnelling electrons, however, prefer the thinner barriers that are the result of tilt to the left. As the temperature is lowered, the tunneling current may exceed that due to thermal excitation, and the total net current reverses direction (From [14]).

2. APPLICATIONS OF BROWNIAN MOTORS AND RATCHETS

In the last few years, ratchets have been experimentally realized in a variety of different systems. A representative overview of the status of experiments in 2002 is provided by a special issue of *Applied Physics A* [19]. Examples include experiments using colloidal particles in electrostatic potentials [16], optically confined particles [20], mercury droplets [21], electrons in semiconductors [22-25], cold atoms [26], and molecules in lipid bilayers [27] and in aqueous solution [28] on patterned surfaces. For a comprehensive overview of theoretical and experimental work on ratchets see the recent review by Peter Reimann [10].

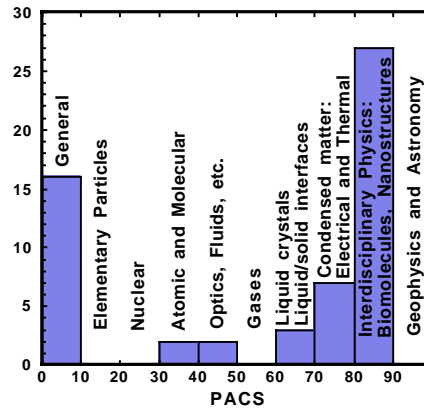
The research field concerned with controlled motility in a Brownian environment, and the concept of Brownian motors, is remarkable interdisciplinary, as highlighted by the variety of backgrounds of researchers contributing to the field. A snapshot of the distribution of experimental work on Brownian motors across the sub-fields of physics is provided by the graph on the next page showing the distribution of PACS numbers as selected by the authors for their respective articles in the recent special issue on Brownian motors mentioned above [19]. The theoretical foundations of Brownian motors in the statistical physics of fluctuations on the one hand, and the strongly multidisciplinary character of experimental work on the other hand, is emphasized by the two peaks at low and at high PACS numbers.

In the oral conference contribution, I will attempt to give a representative overview of experimental work on ratchets in general, and on applications of the concept in particular. However, in this paper I will focus on reviewing some recent work on ratchets for electrons in semiconductor heterostructures.

Nano-fabricated semiconductor devices allow to extend the study of ratchet effects from the classical to the quantum regime, where the particle wave properties, quantum tunneling, or energy quantisation come into play. These effects can usually not be observed in biologically relevant systems, but are of much interest from a fundamental point of view [11, 29]. In particular, we will describe in Section 4 an experimental tunneling ratchet that can sort electrons by their energy [24]. This property can in principle be employed to construct a heat engine [30] based on the ratchet effect, as discussed in Section 5. However, with regard to the biological interest at the present conference, we will

begin in the following Section 3 by mentioning a few aspects of the relation between classical ratchets and biological motor proteins.

It should be noted that the present review is substantially based on a contribution to an earlier SPIE conference [31]. A more complete and more recent review on semiconductor realizations of ratchets and their applications can be found in [32].



Distribution of *Physics and Astronomy Classification Scheme* (PACS) numbers as selected by the authors for their respective articles in a recent special issue on Brownian motors [19]. The peak below 10 indicates the theoretical foundation of Brownian motors in the statistical physics of fluctuations and transport physics. Experimental articles report the use of cold atoms, molecules and electro-hydrodynamic effects (the 30s and 40s), of liquid crystals and fluids (the 60s), and of solid state devices (the 70s). At the high end of the scale, the large group of selected classification numbers between 80 and 90 (Interdisciplinary Physics) represents the theory of biological systems (motor proteins and ion pumps), experiments using bio-molecules, contributions to materials science, as well as the proposal and use of nanoelectronic and of superconducting devices. (From [33]).

3. THE THERMAL RATCHET MODEL AND MOLECULAR MOTORS

One example for a molecular motor that has been proposed to operate similar to a pulsating ratchet is the KIF1A-kinesin. Its task is the transport of filled vesicles along microtubule, linear polymers that form highways inside living cells. Single-molecule, optical microscope studies of fluorescently marked kinesin motors reveal that their motion has a drift component of order 0.1 m/s per second and a smaller stochastic component, measured as a broadening of the distribution of an ensemble of motors over time [34]. The kinesin can be attached to the microtubule in either a weak or a strong binding state. It has been speculated that in the weak binding state the kinesin can diffuse along the microtubule, much like in a groove potential. In the strong binding state, however, it would feel an asymmetric potential provided by the periodic polarized structure of the microtubule segments. Switching between the two states, which have a potential difference of about $4 k_B T$, would occur as part of the hydrolysis cycle of ATP which is present in the cell in a non-equilibrium concentration. In effect, the kinesin would then be able to move along the microtubule in the same fashion as the particles in a pulsating ratchet [34]. The energy required to lift the motor from the strong to the weak binding state would be provided by the hydrolysis of one ATP molecule per cycle, similar to the pulsating ratchet where the energy is provided by the external switching of

the potential. The asymmetry required to define the direction of motion is in this model given by the structure of the microtubule along which the kinesin molecule moves.

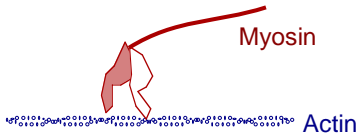


Fig. 3. Cartoon of a myosin motor moving along an actin filament. In a muscle cell, many myosin motors attached to each other form a filament. On flexing a muscle, myosin and actin filaments move relative to each other. For a more realistic illustration, see [35].

Another example for a molecular motor discussed in terms of a Brownian ratchet is the myosin-actin system that effects muscle contraction. Myosin molecules move stepwise along filaments formed by periodically arranged actin (Fig. 3), and exert a force of a few piconewton per myosin molecule [36]. According to a deterministic model, a power-stroke, effected by a shape change of the myosin molecule, pulls the motor along the actin filament by exactly one period per hydrolysed ATP. Recent, advanced single-molecule experiments, however, found evidence that the motion of myosin is more stochastic than one would expect from such a deterministic model. Myosin was found to sometimes hop multiple steps per consumed ATP molecule, and even stochastic backward stepping was observed [5]. These latter findings appear to support a ratchet model of muscle action [37].

It should be noted that a simple ratchet picture does not account for the whole complexity of molecular motors such as myosin and kinesin. The ratchet model should therefore be seen in conjunction with other models (for a recent review, and for animations of kinesin- and myosin-motility, see for instance [35]). An example for a biological mechanism for force generation on a molecular scale that appears to be well described by a ratchet model is the polymerization of actin polymers, which plays a central role in cell motility and cell partition. A stochastic model of the ATP consuming self-assembly of the actin polymer has been shown to account for force generation in front of the growing tip [38, 39].

4. TUNNELLING RATCHETS

We will now return from this brief excursion into biology and turn to semiconductor realizations of ratchets that employ quantum effects for their operation. Quantum effects in ratchets were first studied theoretically by taking into account the possibility of quantum tunnelling through the energy barriers in a rocking ratchet [40]. In the classical regime of transport, the current direction in an adiabatically rocked ratchet is in the direction of the gentler slopes of the potential, because the barrier heights are lower upon linear tilt in this direction (Fig. 1). In the quantum regime however, when tunnelling contributes to the current, not only the *height*, but also the *shape* of the barrier is important. This leads to qualitatively new behaviour, namely a net current direction that depends on temperature. This behaviour can be understood intuitively as follows (Fig. 1): when the saw-tooth barriers are tilted to the left, towards the steeper slopes of the potential, the barriers tend to be thinner at a given energy below the barrier top than for tilt to the right. Consequently, the (time-averaged) net tunnelling current will be to the left, in a direction opposite to that of the net classical current. Which of the two contributions —tunnelling through, or excitation over the barriers — is larger, depends on the energy distribution of the particles. In the high temperature limit, the net current is in general to the right due to thermal excitation. In the low temperature limit, the tunnelling current to the left can be

largest, and the total current can reverse direction as the temperature is decreased [24, 29, 40]. It is also interesting to note that the tunnelling contribution to the current does not go to zero in the zero-temperature limit, unlike the classical current that disappears when thermal excitation is removed altogether [40].

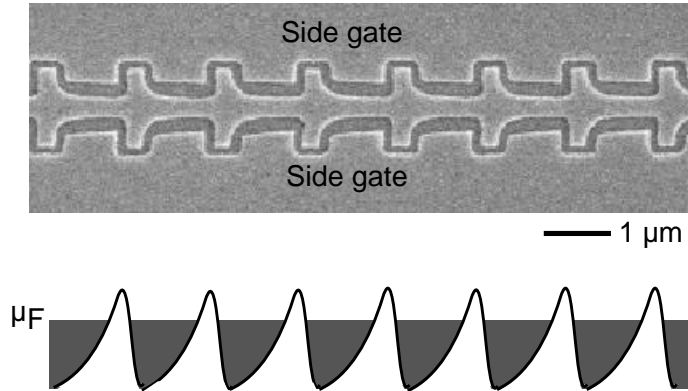


Fig. 4. An electron tunnelling ratchet. The top figure is a scanning electron micrograph (top-view) of an electron wave-guide defined in a GaAs/AlGaAs heterostructure by electron beam lithography and shallow wet etching. The lower figure indicates the ratchet potential experienced by one-dimensional electrons traversing the channel.

In Figure 4 a scanning electron micrograph of an experimental tunnelling ratchet for electrons is shown. The top-view shows an etched pattern on the surface of a semiconductor heterostructure. About a hundred nanometer under the surface a thin, conducting sheet of electrons is situated at an interface of GaAs and AlGaAs. This sheet forms a so-called two-dimensional electron gas (2DEG), meaning that electrons can move within the plane of the image, but motion in the third dimension is limited to the lowest quantised energy value due to electrostatic confinement in this dimension. Etched trenches that were defined by electron-beam lithography and shallow wet etching, visible as darker lines in the image, electrostatically deplete the 2DEG underneath, confining the electrons into a narrow channel. The lithographic width of this channel has been chosen to be about 100 nm at the narrowest points, corresponding to just a few electron Fermi wave lengths ($\lambda_F \sim 40$ nm). The channel therefore effectively forms a one-dimensional (1D) electron wave-guide. The effective, electrostatic width of the wave-guide can be further reduced by negatively charging the electron sheet regions parallel to the channel, using them as side-gates. A more negative side gate voltage V_g corresponds to a narrower channel and therefore higher potential barriers (for further details, see [24]). When the width of the channel is reduced such that the narrowest parts are only about $\lambda_F/2$ wide, then only the lowest 1D wave mode contributes to transport through the channel. The energy variation of this wave mode along the channel is also indicated in Fig. 4 - an electron moving along the channel experiences each of the periodic constrictions as an asymmetric energy barrier, and a periodic, asymmetric tunnelling ratchet potential is formed. The lateral dimensions of each ratchet cell were much smaller than the length scales for elastic (6 μm) and inelastic (> 10 μm) scattering at the temperatures and voltages used here (energies $k_B T$ and $|eV| \dagger 1$ meV, where k_B is Boltzmann's constant and e is the electron charge).

Using Ohmic contacts situated far away to the left and right of the channel as source and drain contacts (not visible in Fig. 4), a voltage can be applied along the channel. The resulting current I is determined by the barriers's reflection and tunnelling coefficients and is sensitive to the precise shape of these barriers. Because of the geometric asymmetry, the electric field along the channel produced by the voltage V deforms the barriers in a way that depends on the polarity of V , such that $I(V) \neq -I(-V)$. In order to rock the ratchet we used here a square-wave source-drain voltage of amplitude V_0 . The frequency was chosen to be much slower than all electronic time-scales, such as energy relaxation times (so-called adiabatic rocking). The electronic system was therefore in equilibrium at all times, and to

understand the ratchet behaviour it is sufficient to analyse the two DC situations V_0 and $-V_0$. Transient behaviour can be neglected and the time-averaged, net current induced by the rocking is given by $I_{\text{net}} = 0.5 [I(V_0) + I(-V_0)]$.

Under conditions when the barrier height approximately matches the Fermi energy $\mu_F = 11.8$ meV, one can observe a reversal of the net current direction as a function of the temperature, while all other parameters, including the shape and height of the potential barriers, are kept constant (Fig. 5). The data shown here were obtained using a rocking voltage $V_0 = 1$ mV corresponding to a voltage drop of 0.1 mV over each barrier (less than 1% of μ_F) in the device shown in Fig 4, which consisted of 10 ratchet barriers in total. The net current generated in this way corresponds to about 1 to 5 % rectification of the total current and, at 4 K, was initially positive but reversed its direction as the temperature was reduced to 0.4 K.

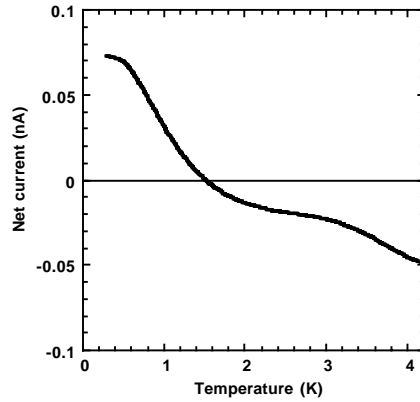


Fig. 5. Measured net current, induced by rocking the ratchet potential of Fig. 4 by a square-wave voltage of amplitude 1 mV, versus temperature. (Data from [24])

To provide an intuitive understanding of this temperature-induced current reversal, a model of 1D transport over a single ratchet barrier situated between two 2D electron reservoirs R and L is used (Fig. 6), where the barrier shape is based on the geometry of the device in Fig. 4. We assume that transport is ballistic, no inelastic processes occur, and we consider electron transport only in the lowest one-dimensional subband (assuming that any higher subbands are not populated at the narrowest points of the wave-guide). At low temperatures ($k_B T \ll \mu_F - |eV_0|$), the electric current driven by a bias voltage V (applied between the 2DEG reservoirs at either end of the channel) is given by a Landauer equation [41],

$$I = \frac{2e}{h} \int_{-\mu_{av}}^{\infty} t(\epsilon, V) [f_R(\epsilon, V) - f_L(\epsilon, V)] d\epsilon. \quad (1)$$

Here, $f_{L/R}(\epsilon, T_{L/R}) = 1/(1+\exp[(-\epsilon-eV/2)/k_B T_{L/R}])$ are the Fermi distribution functions in the electron reservoirs to the left (L) and right (R) of the barrier and ϵ is the energy of the electrons relative to $\mu_{av} = 0.5(\mu_L + \mu_R)$ (Note that $\mu_{av} = \mu_F$ for $V \rightarrow 0$). Further, $e = +1.6 \cdot 10^{-19}$ C, and $t(\epsilon, V)$ is the probability that electrons are transmitted by the device. We assume here that $|eV| \ll \mu_{av}$, which allows us to use $-\mu_{av}$ as the lower limit of integration, independent of the voltage sign.

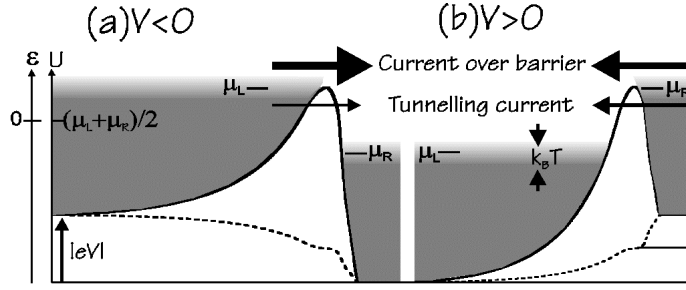


Fig. 6. A single ratchet energy barrier as used in the model. The shape of the barrier is based on the lithographic shape of the electron wave-guide in Fig. 4. To obtain the barrier at finite negative (a) or positive (b) voltage, an assumption for the spatial distribution of the voltage drop needs to be made (dashed line). (Illustration from [30].)

The origin of a ratchet effect in the present system is the deformation of the barrier shape by an external electric field, inducing a voltage dependence of $t(\epsilon)$. In the experimental wave guide (Fig. 4), energy barriers are formed at each constriction of the wave guide due to the lateral confinement of the electron waves. From the lithographic shape of the channel one can therefore estimate the form of the energy barriers, as shown in Fig. 6 (for details see [24]). To obtain the barrier shape at finite voltage the spatial distribution of the voltage drop needs to be known, which self-consistently depends on screening effects. Here we assume a spatial distribution of the voltage drop that is proportional to the local derivative of the barrier (Fig. 6). This model is based on the observation that a more rapid potential variation leads to stronger wave-reflection, and therefore a locally more rapid voltage drop. This particular choice has the desirable side-effect that the barrier height remains independent of the sign of the voltage, resulting in the suppression of a classical contribution to the net current.

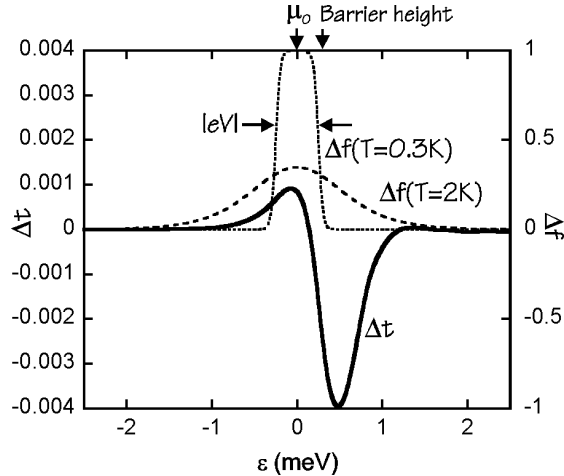


Fig. 7. Bold line: the difference in the transmission functions for positive and negative bias voltage for the potential barrier in Fig. 6. Dashed lines: The Fermi window \tilde{f} , that is, the range of electron energies which contribute to the current (see text for further details). (Illustration from [30].)

The net current can be written as [24]:

$$I^{net} = \frac{e}{h} \int_{-\mu_{av}}^{\infty} \Delta t(\epsilon, V_0) \Delta f(\epsilon, V_0) d\epsilon \quad (2)$$

where $\Delta f(\epsilon, V_0) \equiv f_R(\epsilon, V_0) - f_L(\epsilon, V_0)$ is the Fermi window, the range of electron energies which contribute to the current. The term $\Delta t(\epsilon, V_0) \equiv t(\epsilon, V_0) - t(\epsilon, -V_0)$ is the difference between the transmission probabilities for positive and negative voltages and is shown in Fig. 7. For $V_0 = 0.5$ mV, we find that $\tilde{f}(\epsilon)$ is of the order of 10^{-3} , for energies within a few millielectron volts of the barrier height used in the model, $E = 12.0$ meV (Fig. 7). The energy window

$\tilde{f}(\epsilon)$ is shown in Fig. 7 for $V_0 = 0.5$ mV, $\mu_F = 11.7$ meV and three different temperatures. Electrons with energies smaller than the barrier height are more likely to tunnel from right to left ($V = V_0$) when the barrier becomes thinner, than from left to right ($V = -V_0$) when the barrier becomes thicker. This results in Δt being positive in this energy range. For energies above the barrier height the situation is reversed: electron wave reflection is stronger for steep, thin barriers (for $V = V_0$) than for the smoother, thicker barrier ($V = -V_0$), and Δt is negative in that energy range. As Δf is adjusted (through changing T , V_0 or the Fermi energy) to sample the Δt curve where it is negative rather than positive, the net current reverses direction.

5. QUANTUM HEAT PUMPS

In the following, we will concentrate on a direct consequence of the behaviour just described: namely, ratchets in which the net current direction depends on temperature act as heat pumps. This is easiest to see by considering the situation where the net current goes through zero — that is, when the net particle flow due to tunnelling, flowing at low energies, is exactly counterbalanced by the thermally excited net current flowing at higher energies (Figs. 4, 5). Clearly, a net effect of the ratchet action is then the pumping of heat. In the more general case, when the net particle current may be finite, the heat flow due to the ratchet's heat pumping action is superimposed on the net energy current that trivially accompanies any finite particle current.

To derive the heat current that accompanies the charge current (Eq. (2)) we note that the heat added when one electron is transferred to a reservoir with chemical potential μ is given by $\Delta Q = (\Delta U - \mu)$, where \mathcal{U} is the internal energy associated with the electron. We consider again the single ratchet barrier of Fig. 6, connecting two 2D electron reservoirs, L and R. The change in heat in L and R upon transfer of one electron from the right to the left is given by $\Delta Q_{L/R} = -[\epsilon + (\mu_L + \mu_R)/2 - \mu_{L/R}] = -(\epsilon \pm eV/2)$. By replacing in Eq. (1) the electron charge, $-e$, by a factor of $\Delta Q_{L/R}$ inside the integral, the heat current can then be written as

$$q_{L/R} = m \frac{2}{h} \int_{-\mu_{av}}^{\infty} (\epsilon \pm eV/2) t(\epsilon, V) \Delta f(\epsilon, V) d\epsilon. \quad (3)$$

Note that $q_L(V)$ exceeds the heat current out of R, $-q_R(V)$, by IV , the Joule heating power supplied by the external bias voltage. The *net* (time-averaged) heat current into the left and right reservoirs can then be written as:

$$\begin{aligned} q_{L/R}^{net} &= 0.5 [q_{L/R}(V_0) + q_{L/R}(-V_0)] \\ &= m \frac{1}{h} \int_{-\mu_{av}}^{\infty} \epsilon \Delta t \Delta f d\epsilon + \frac{1}{h} \frac{eV_0}{2} \int_{-\mu_{av}}^{\infty} \tau \Delta f d\epsilon \\ &= m \frac{1}{2} \Delta E + \frac{1}{2} \Omega \end{aligned} \quad (4)$$

Here $\tau(\epsilon, V_0) = 0.5 [t(\epsilon, +V_0) + t(\epsilon, -V_0)]$ is the average transmission probability for $V = V_0$ and $V = -V_0$. $\Delta E = q_L^{net} - q_R^{net}$ is the heat pumped from the left to the right sides of the device due to the energy sorting properties of the ratchet. Ω can be finite only when $\tau > 0$, that is, for asymmetric, ratchet barriers. $\%_0 = q_L^{net} + q_R^{net}$ is the electrical power input (Joule heating), averaged over one cycle of rocking.

One can interpret Eq. (4) as follows: $\%_0$ is the waste heat generated by operating the ratchet as a heat pump, and both reservoirs receive the same share, $\%_0/2$ each. Part of this heat, the amount $\Omega/2$, is then removed by the heat pumping action of the ratchet from one reservoir, and is added to the other reservoir. In this sense, the ratchet acts as a badly constructed refrigerator - it cools one reservoir, but deposits half of the waste heat in the same reservoir.

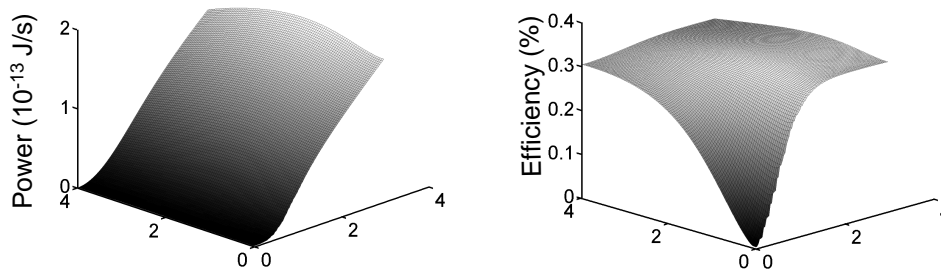


Fig. 8. The heat pumping power (left) and efficiency (right) versus temperature in K (left hand axis) and rocking voltage in meV (right hand axis) of the ratchet barrier of Fig. 6 for parameter values where the particle current goes through zero. (Adapted from [21].)

When $|\tilde{E}| < \epsilon_0$, both reservoirs are heated, but one more than the other. Cooling of one reservoir takes place when $|\tilde{E}| > \epsilon_0$.

Calculated values of \tilde{E} for the model potential Fig. 6 are shown in Fig. 8 for sets of parameters where the electric current goes through zero. Limiting the analysis to these parameters avoids the trivial situation where \tilde{E} is enhanced by a finite net particle current. The power goes to zero for small bias voltage — this is the linear response limit where, by definition, the ratchet cannot work. Also shown in Fig. 8 is the coefficient of performance $\chi = |\tilde{E}|/\epsilon_0$ for the ratchet as a heat pump. The coefficient of performance is positive, indicating that heat is pumped from left to right for the range of parameters used in the calculation. The very small value of χ originates from the fact that much more heat is deposited in each reservoir due to ohmic heating than is pumped by the ratchet. This low efficiency is a result of the fact that the potential barrier of Fig. 6 transmits electrons in a wide range of energies in both rocking directions (all of which contribute to heating), while the ratio $\Delta t/\tau$ is less than 1%.

Using sharp energy filters, such as resonant tunnelling barriers [42, 43], potentials where $\Delta t/\tau \cong 1$ can be realized. Cooling of one reservoir, that is, a coefficient of performance $\chi > 1$ can then be achieved in principle, which opens interesting avenues to experimental realisations of mesoscopic heat pumps.

Most interestingly, the possibility to filter electrons according to their energy using, for instance, resonant tunneling barriers, can also be used to render electron heat engines and/or refrigerators reversible. That is, it is possible in principle to operate arbitrarily closely to the Carnot efficiency. This concept is described in detail in [44].

ACKNOWLEDGEMENTS

This work was supported by the Australian Research Council and by the University of Oregon. The author is grateful to Tammy Humphrey, Anneli Lfgren, Richard Newbury, P r Omling, Alexander Sushkov, and Richard P. Taylor for their fruitful collaboration and for their crucial contributions to this work.

REFERENCES

1. E. M. Purcell, *American Journal of Physics* **45**, 3 - 11 (1977).
2. S. Vogel, *Life in Moving Fluids* (Princeton University Press, Princeton, NJ, 1996).
3. T. Strick, J.-F. Allemand, V. Croquette, and D. Bensimon, *The Manipulation of Single Biomolecules*, *Physics Today*, October 2001, 46-51
4. K. Kinosita, R. Yasuda, H. Noji, S. Ishiwata, and M. Yoshida, *Cell* **93**, 21 (1998).
5. K. Kitamura, M. Tokunaga, A. H. Iwane, and T. Yanagida, *Nature* **397**, 129-134 (1999).
6. M. O. Magnasco, *Phys. Rev. Lett.* **71**, 1477 (1993).
7. P. H nggi and R. Bartussek, in *Nonlinear Physics of Complex Systems - Current Status and Future Trends*, edited by J. Parisi, S. C. M ller and W. Zimmermann (Springer, Berlin, 1996).
8. F. J licher, A. Ajdari, and J. Prost, *Rev. Mod. Phys.* **69**, 1269 (1997).
9. R. D. Astumian, *Science* **276**, 917 (1997).
10. P. Reimann, *Phys. Rep.* **361**, 57 - 265 (2002).
11. R. D. Astumian, *Making molecules into motors*, *Sci. Am.*, July 2001, 57-64
12. P. Reimann and P. H nggi, *Appl. Phys. A* **75**, 169 - 178 (2002).
13. R. D. Astumian and P. H nggi, *Brownian Motors*, *Physics Today*, November 2002, 33-39
14. H. Linke, *Von D monen und Elektronen* , *Phys. Bl.*, May 2000, 45-47
15. J. Prost, J.-F. Chauwin, L. Peliti, and A. Ajdari, *Phys. Rev. Lett.* **72**, 2652-2655 (1994).
16. J. Rousselet, L. Salome, A. Ajdari, and J. Prost, *Nature* **370**, 446 (1994).
17. R. Ketzmerick, M. Wei, and F.-J. Elmer, *Brownian Motor*, http://www.chaos.gwdg.de/java_gallery/brownian_motor/bm.html, <http://monet.physik.unibas.ch/~elmer/bm>.
18. R. Bartussek, P. H nggi, and J. G. Kissner, *Europhys. Lett.* **28**, 459 (1994).
19. H. Linke (Ed.): *Special issue: Ratchets and Brownian motors: basics, experiments and applications*, *Applied Physics A* (Springer, 2002), Vol. 75 (2), p 167-352.
20. L. P. Faucheux, L. S. Bourdieu, P. D. Kaplan, and A. J. Libchaber, *Phys. Rev. Lett.* **74**, 1504 (1995).
21. L. Gorre, E. Ioannidis, and P. Silberzan, *Europhys. Lett.* **33**, 267 (1996).
22. A. M. Song, A. Lorke, A. Kriele, J. P. Kotthaus, W. Wegscheider, and M. Bichler, *Phys. Rev. Lett.* **80**, 3831 (1998).
23. H. Linke, W. Sheng, A. L fgren, H. Xu, P. Omling, and P. E. Lindelof, *Europhys. Lett.* **44**, 341-347 (1998).
24. H. Linke, T. E. Humphrey, A. L fgren, A. O. Sushkov, R. Newbury, R. P. Taylor, and P. Omling, *Science* **286**, 2314 - 2317 (1999).

25. A. M. Song, P. Omling, L. Samuelson, W. Seifert, and I. Shorubalku, *Appl. Phys. Lett.* **79**, 1357-1359 (2001).
26. C. Mennerat-Robilliard, D. Lucas, S. Guibal, J. Tabosa, C. Jurcak, J.-Y. Courtois, and G. Grynberg, *Phys. Rev. Lett.* **82**, 851 (1999).
27. A. v. Oudenaarden and S. G. Boxer, *Science* **285**, 1046-1048 (1999).
28. C.-F. Chou, O. Bakajin, S. W. P. Turner, T. A. J. Duke, S. S. Chan, E. C. Cox, H. G. Craighead, and R. H. Austin, *PNAS* **96**, 13762-13765 (1999).
29. M. Brooks, *Quantum Clockworks*, *New Scientist*, 22 January 2000, 28-31
30. T. E. Humphrey, H. Linke, and R. Newbury, *Physica E* **11**, 281 - 286 (2001).
31. H. Linke and T. E. Humphrey, *Proceedings of SPIE* **4590**, 263 (2001).
32. H. Linke and A. M. Song, in *Electron Transport in Quantum Dots* (Kluwer, 2003).
33. H. Linke, *Appl. Phys. A* **75**, 167 (2002).
34. Y. Okada and N. Hirokawa, *Science* **283**, 1152 - 1155 (1999).
35. R. D. Vale and R. A. Milligan, *Science* **288**, 88-95 (2000).
36. B. Alberts, D. Bray, J. Lewis, M. Raff, K. Roberts, and J. D. Watson, *Molecular Biology of the Cell* (Garland Publishing, New York, 1994).
37. T. Yanagida, *Muscling in*, *Sci. Am.*, July 2001, 64
38. A. Mogilner and G. Oster, *Biophys. J.* **71**, 3030-3045 (1996).
39. A. v. Oudenaarden and J. A. Theriot, *Nature Cell Biology* **1**, 493-499 (1999).
40. P. Reimann, M. Grifoni, and P. H nggi, *Phys. Rev. Lett.* **79**, 10 (1997).
41. S. Datta, *Electronic Transport in Mesoscopic Systems* (Cambridge University Press, Cambridge, 1995).
42. H. L. Edwards, Q. Niu, and A. L. de Lozanne, *Appl. Phys. Lett.* **63**, 1815 (1993).
43. H. L. Edwards, Q. Niu, G. A. Georgakis, and A. L. de Lozanne, *Phys. Rev. B* **52**, 5714-5736 (1995).
44. T. E. Humphrey, R. Newbury, R. P. Taylor, and H. Linke, *Phys. Rev. Lett.* **89**, 116801 (2002).